

# Strong-coupling effects in the relaxation dynamics of ultracold neutral plasmas

T. Pohl and T. Pattard

October 2, 2018

Max Planck Institute for the Physics of Complex Systems,  
Nöthnitzer Str. 38, D-01187 Dresden, Germany

## Abstract

We describe a hybrid molecular dynamics approach for the description of ultracold neutral plasmas, based on an adiabatic treatment of the electron gas and a full molecular dynamics simulation of the ions, which allows us to follow the long-time evolution of the plasma including the effect of the strongly coupled ion motion. The plasma shows a rather complex relaxation behavior, connected with temporal as well as spatial oscillations of the ion temperature. Furthermore, additional laser cooling of the ions during the plasma evolution drastically modifies the expansion dynamics, so that crystallization of the ion component can occur in this nonequilibrium system, leading to lattice-like structures or even long-range order resulting in concentric shells.

## 1 Introduction

Experiments in cooling and trapping of neutral gases have paved the way toward a new parameter regime of ionized gases, namely the regime of ultracold neutral plasmas (UNPs). Experimentally, UNPs are produced by photoionizing a cloud of laser-cooled atoms collected in a magneto-optical trap [1], with temperatures down to 10  $\mu\text{K}$ . By tuning the frequency of the ionizing laser, initial electron kinetic energies of  $E_e/k_B = 1\text{K} - 1000\text{K}$  have been achieved. The time evolution of several quantities characterizing the state of the plasma, such as the plasma density [1, 2, 3], the rate of expansion of the plasma cloud into the surrounding vacuum [2], the energy-resolved population of bound Rydberg states formed through recombination [4], or electronic [5, 6] as well as ionic [3] temperature have been measured using various plasma diagnostic methods.

Despite the low typical densities of  $\approx 10^9 \text{ cm}^{-3}$ , the very low initial temperatures suggest that these plasmas have been produced well within the strongly coupled regime, with Coulomb coupling parameters up to  $\Gamma_e = 10$  for the electrons and even  $\Gamma_i = 30000$  for the ions. Thus, UNPs seem to offer a unique opportunity for a laboratory study of neutral plasmas where, depending on the initial electronic kinetic energy, either one component (namely the ions) or both components (ions and electrons) may be strongly coupled. Moreover, the plasma is created in a completely uncorrelated state, i.e. far away from thermodynamical equilibrium. The relaxation of a strongly correlated system towards equilibrium is an interesting topic in non-equilibrium thermodynamics and has been studied for decades. The history of this problem must be traced back to the important contributions of Klimontovich [7, 8, 9], who pointed out that kinetic energy conserving collision integrals such as the Boltzmann, Landau and Lenard-Balescu collision integrals are not appropriate

for such a situation, and derived non-Markovian kinetic equations taking correctly into account total energy conservation of the system. In the following years this problem has attracted much attention and the relaxation of nonequilibrium strongly coupled plasmas has been studied by a variety of different methods [10, 11, 12, 13]. The very low densities of UNPs make it now possible to directly observe the dynamical development of spatial correlations, which may serve as the first experimental check of the present understanding of the strongly coupled plasma dynamics. Moreover, it turns out that the timescale of the plasma expansion, the correlation time as well as the relaxation time of the ions are almost equal. Therefore Bogoliubov’s functional hypothesis, usually used in kinetic theory, breaks down under the present conditions, which may lead to a very interesting relaxation behavior but also causes some difficulties in the theoretical description of these systems, since the plasma dynamics can not be divided into different relaxation stages.

## 2 Theoretical approach

A full molecular dynamics simulation of ultracold neutral plasmas over experimentally relevant timescales is infeasible with present-day computer resources due to the large number of particles ( $N \approx 10^5$ ) and the long observation times ( $t \approx 10^{-4}$  s) involved. In order to model the evolution of UNPs, we have developed a hybrid molecular dynamics (HMD) approach which treats electrons and ions on different levels of sophistication, namely in a hydrodynamical approximation on the one hand (for the electrons) and on a full molecular dynamics level on the other hand (for the ions) [14]. For the electrons, it has been shown that several heating effects, such as continuum threshold lowering [15], build-up of correlations [16], and, predominantly, three-body recombination [17] rapidly increase the electronic temperature. As a consequence, the electrons are always weakly coupled,  $\Gamma_e < 0.2$ , over the whole course of the system evolution. Moreover, due to the small electron-to-ion mass ratio, the relaxation timescale of the electrons is much smaller than that of the ions as well as the timescale of the plasma expansion. Hence, an adiabatic approximation may safely be applied, assuming instant equilibration of the electrons. This allows for the use of much larger timesteps than in a full MD simulation since the electronic motion does not need to be resolved. It is this adiabatic approximation for the electrons which makes a molecular dynamics treatment of the ionic motion in UNPs computationally feasible. The electronic density is determined self-consistently from the Poisson equation. The fact that the potential well created by the ions which is trapping the electrons has a finite depth is taken into account by using a King-type distribution [18] known from simulations of globular clusters rather than a Maxwell-Boltzmann distribution for the electron velocities, with the electronic temperature  $T_e$  obtained from energy conservation. The finite well depth also leads to evaporation of a fraction of the free electrons in the very early stage of the plasma evolution, which is accounted for by determining the fraction of trapped electrons from the results of [1]. The dynamics of the heavy particles is described in the framework of a chemical picture, where inelastic processes, namely three-body recombination and electron impact ionization, excitation and deexcitation, are taken into account on the basis of Boltzmann-type collision integrals [19, 9], with the transition rates taken from [20]. Numerically, the resulting collision integrals are evaluated using a Monte Carlo sampling as described in [21, 14, 22]. The ions and recombined atoms are then propagated individually in a molecular dynamics simulation, taking into account the electronic mean-field potential and

the full interaction potential of the remaining ions<sup>1</sup>. In order to allow for larger particle numbers, the most time-consuming part of the HMD simulation, namely the calculation of the interionic forces, is done using a treecode procedure originally designed for astrophysical problems [23], which scales like  $N_i \ln N_i$  rather than  $N_i^2$  with the number  $N_i$  of ions.

As shown in several publications [14, 24, 25, 22], the HMD approach outlined above provides a powerful method for the description of UNPs, taking full account of ionic correlation effects. However, due to the large numerical effort involved, it is limited to particle numbers of  $N_i \approx 10^5$ . While this permits a direct simulation of many, particularly of the early, experiments, an increasing number of experiments is performed with larger particle numbers up to  $10^7$ . Thus, an alternative method which is able to treat such larger systems is desirable. Such a method is indeed available [14], based on a hydrodynamical description of both electrons and ions similar to that introduced in [17, 21]. Starting from the first equation of the BBGKY hierarchy, one obtains the evolution equations for the one-particle distribution functions  $f$  of the electrons and ions. Neglecting again electron-electron as well as electron-ion correlations, and employing the same adiabatic approximation for the electrons already used in the HMD approach, a quasineutral approximation [26] permits expressing the mean-field electrostatic potential in terms of the ionic density, leading to a closed equation for the ion distribution function which contains the electron temperature as a parameter. A Gaussian ansatz for the ion distribution function,

$$f_i \propto \exp\left(-\frac{r^2}{2\sigma^2}\right) \exp\left(-\frac{m_i(\mathbf{v} - \gamma\mathbf{r})^2}{2k_B T_i}\right), \quad (1)$$

which corresponds to the initial state of the plasma cloud, is then inserted into the evolution equations for the second moments  $\langle r^2 \rangle$ ,  $\langle \mathbf{r}\mathbf{v} \rangle$  and  $\langle v^2 \rangle$  of the ion distribution function. In this way, evolution equations for the width  $\sigma$  of the cloud, the parameter  $\gamma$  of the hydrodynamical expansion velocity  $\mathbf{u} = \gamma\mathbf{r}$  and the ionic temperature  $T_i$  are obtained. Ionic correlations are taken into account in an approximate way using a local density approximation together with a gradient expansion, reducing the description of their influence on the plasma dynamics to the evolution of a single macroscopic quantity, namely the correlation energy  $U_{ii}$  of a homogeneous plasma. The relaxation behavior of  $U_{ii}$  is modeled using a correlation-time approximation [27] with a correlation time equal to the inverse of the ionic plasma frequency,  $\tau_{\text{corr}} = \omega_{p,i}^{-1}$ , together with an analytical expression for the equilibrium value of  $U_{ii}$  [28]. Finally, inelastic processes such as three-body recombination and electron impact ionization, excitation and deexcitation are incorporated on the basis of rate equations, and the influence of the recombined Rydberg atoms on the expansion dynamics is taken into account assuming equal hydrodynamical velocities

---

<sup>1</sup>In order to bring out clearly the role of ionic correlations, it is also possible to neglect them in the HMD approach by propagating the ions in the mean-field potential created by all charges rather than the full ionic interaction.

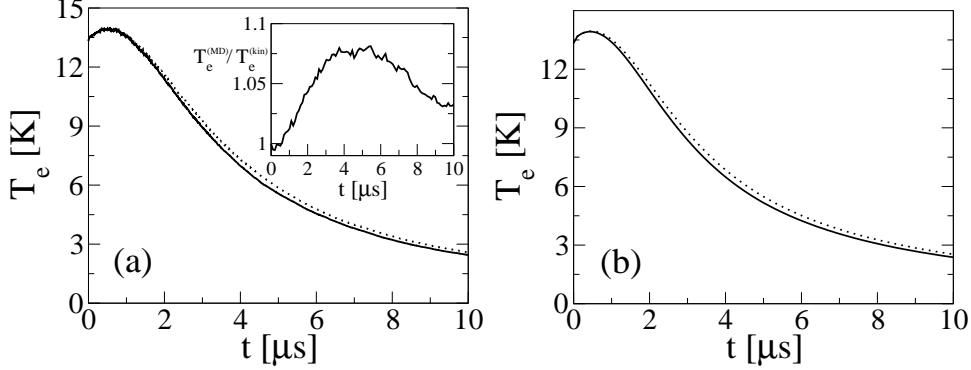


Figure 1: Electronic temperature  $T_e(t)$  for an expanding plasma of 40000 Sr ions with an initial average density of  $\rho_i = 10^9 \text{cm}^{-3}$  and an initial electron kinetic energy of 20 K, obtained from the HMD simulation (a) and from eqs. (2) (b), with (solid) and without (dotted) the inclusion of ionic correlations. The inset shows the ratio of the electron temperatures obtained from both methods.

for atoms and ions. The final set of evolution equations then reads

$$\dot{\sigma} = \gamma\sigma, \quad (2a)$$

$$\dot{\gamma} = \frac{N_i (k_B T_e + k_B T_i + \frac{1}{3} U_{ii})}{(N_i + N_a) m_i \sigma^2} - \gamma^2, \quad (2b)$$

$$k_B \dot{T}_i = -2\gamma k_B T_i - \frac{2}{3} \gamma U_{ii} - \frac{2}{3} \dot{U}_{ii}, \quad (2c)$$

$$\dot{U}_{ii} = -\omega_{p,i} (U_{ii} - U_{ii}^{(eq)}) \quad (2d)$$

$$\begin{aligned} \dot{\mathcal{N}}_a(n) = & \sum_{p \neq n} [R_{bb}(p, n) \mathcal{N}_a(p) - R_{bb}(n, p) \mathcal{N}_a(n)] \\ & + R_{tbr}(n) N_i - R_{ion}(n) \mathcal{N}_a(n) \end{aligned} \quad (2e)$$

and the electronic temperature is determined by energy conservation,

$$N_i k_B T_e + [N_i + N_a] [k_B T_i + m_i \gamma^2 \sigma^2] + \frac{2}{3} N_i U_{ii} - \frac{2}{3} \sum_n \mathcal{N}_a(n) \frac{\mathcal{R}}{n^2} = \text{const.}, \quad (2f)$$

where  $\mathcal{N}_a(n)$  defines the population of Rydberg states,  $N_a = \sum_n \mathcal{N}_a(n)$  is the total number of atoms and  $\mathcal{R} = 13.6 \text{eV}$  is the Rydberg constant.

The preceding hydrodynamical method is much more approximate than the HMD approach, but, on the other hand, it is much simpler and quicker. For particle numbers of  $N_i \approx 10^5$ , it requires about two orders of magnitude less CPU time. Since its computational effort is independent of the number of particles, it allows for a simulation of larger plasma clouds corresponding to a number of current experiments. Moreover, and maybe equally important, it provides physical insight into the plasma dynamics since it is based on a few simple evolution equations for the macroscopic observables characterizing the state of the plasma. As we have investigated in detail in [14], there is generally surprisingly good agreement between the hydrodynamical simulation and the more sophisticated HMD calculation as long as macroscopic, i.e. spatially averaged, quantities such as electronic temperature, expansion velocity, ionic correlation energy etc. are considered. As an example, we show in figure 1 the time evolution of the electronic temperature for a plasma of 40000 Sr ions with an initial average density of  $10^9 \text{cm}^{-3}$  and an initial electron kinetic energy of 20 K, obtained from the HMD simulation (a) and from eqs. (2)

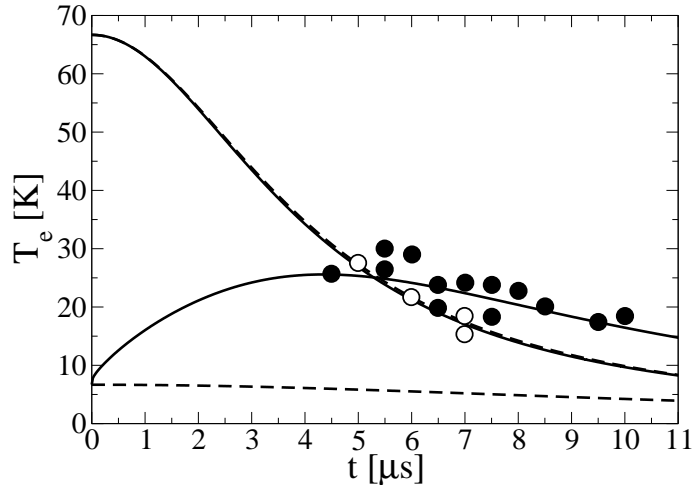


Figure 2: Electronic temperature  $T_e(t)$  for a plasma of  $1.2 \cdot 10^6$  Xenon ions with an initial average density of  $1.35 \cdot 10^9 \text{cm}^{-3}$  for two different initial electron temperatures,  $T_e = 6.67\text{K}$  (filled dots) and  $T_e = 66.67\text{K}$  (open dots). The lines show the hydrodynamical simulation (solid lines: including inelastic collisions, dashed lines: without inelastic collisions), the dots the experiment [5], scaled down by 26% (see text).

(b). During the whole system evolution, the agreement between the two simulation methods is better than about 8%, and it becomes even better at later times. Thus, we conclude that, for the present type of experimental setups, the hydrodynamical method outlined above, and in particular the approximate treatment of ionic correlations, is well suited for the description of the behavior of UNPs.

### 3 Results and discussion

#### 3.1 Comparison with experiments

In fact, fig. 1 only shows good agreement between the two theoretical simulation methods, without comparison with experiment. Such a comparison is now also possible, since measurements of the electron temperature dynamics have recently been reported in [5]. Fig. 2 shows the time evolution of the electronic temperature for a Xenon plasma with  $N_i(0) = 1.2 \cdot 10^6$ ,  $\rho_i(0) = 1.35 \cdot 10^9 \text{cm}^{-3}$  and two different initial temperatures of  $T_e(0) = 66.67\text{K}$  and  $T_e(0) = 6.67\text{K}$ . In addition to the full hydrodynamical simulation according to equations (2), fig. 2 also shows corresponding calculations where the effect of inelastic electron-ion collisions, eq. (2e), is neglected (dashed lines). (The plasmas in these experiments are too large to be simulated using the HMD approach.) For the high initial temperature, there is close agreement between the two corresponding simulations, showing that inelastic processes are almost negligible in this case. Indeed, it is known that the high-temperature plasma expansion is well described by the collisionless plasma dynamics, and the hydrodynamical model is expected to accurately reproduce the plasma dynamics in this regime. Since an overall systematic error of about 70% for the temperature measurement has been reported in [5], we have exploited this fact to calibrate the measured temperatures by scaling down both experimental data sets by 26% in order to match the high-temperature results to our calculations. As can be seen in the figure, there is excellent agreement between simulation and ex-

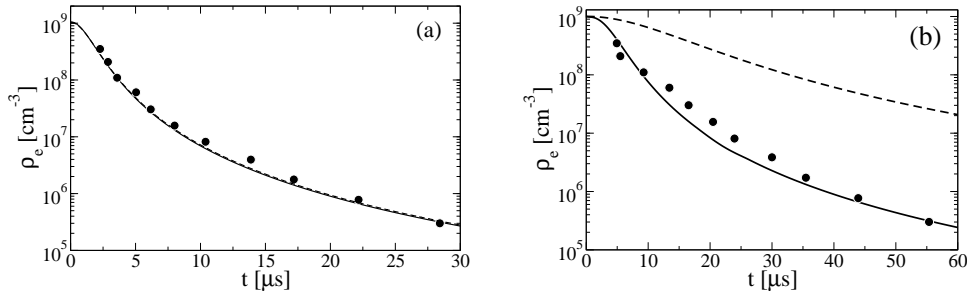


Figure 3: Time evolution of the average electron density of a Xenon plasma of 500000 ions with an initial average density of  $10^9 \text{cm}^{-3}$  and an initial electron temperature of  $T_e = 210\text{K}$  (a) and  $T_e = 2.6\text{K}$  (b). The lines show the results of the model equations (2) (solid lines: including inelastic collisions, dashed lines: without inelastic collisions) and the dots the experimental data from [2].

periment also for the lower temperature. (We stress that there is no further scaling of the low-temperature data in order to achieve quantitative agreement, the same calibration factor as in the high-temperature case is used.) In this case, inelastic collisions play a decisive role for the evolution of the system. More specifically, as has been found already in [17], three-body recombination heats the plasma and significantly changes its behavior, leading to a weakly coupled electron gas, as discussed above in connection with the omission of electronic correlation effects in the numerical treatment. Moreover, there has been some discussion in the literature whether the collision rates of [20] would still be applicable at these ultralow temperatures, or whether three-body recombination would be significantly altered. The close agreement between the present simulation and the experimental data in fig. 2 suggests that the rates of [20], while ultimately diverging  $\propto T_e^{-9/2}$  for  $T_e \rightarrow 0$ , still adequately describe three-body recombination processes in the temperature range under consideration.

As a second example, figure 3 shows the time evolution of the electronic density for a Xenon plasma of 500000 ions with an initial average density of  $10^9 \text{cm}^{-3}$  and two different initial electron temperatures of  $T_e(0) = 210\text{K}$  and  $T_e(0) = 2.6\text{K}$  [2]. Again, it can be seen that the model equations nicely reproduce the density evolution in both temperature regimes, in agreement with [17] where it was shown that the low-temperature enhancement of the expansion velocity [2] is caused by recombination heating and is not due to strong-coupling effects of the electrons.

### 3.2 Role of ionic correlations

Having thus established the validity of our numerical methods for the description of UNPs, we can now turn to a more detailed investigation of the role of ionic correlations in these systems. It is found that, for situations corresponding to the type of experiments [1, 5, 6], they hardly influence the macroscopic expansion behavior of the plasma. This becomes evident, e.g., in fig. 1, where the “full” simulations as described above (solid lines) are compared to a mean-field treatment of the system completely neglecting correlation effects (dotted lines). The correlation-induced heating of the ions [29, 30, 31] leads to a slightly faster expansion of the plasma, which in turn results in a slightly faster adiabatic cooling of the electrons [14]. However, the overall effect is almost negligible.

A closer look, on the other hand, reveals that certain aspects of the expansion dynamics are indeed significantly affected by the strong ion-ion interaction, as can be seen in figure 4. There, the spatial density of the ions is shown after  $t = 3 \mu\text{s}$

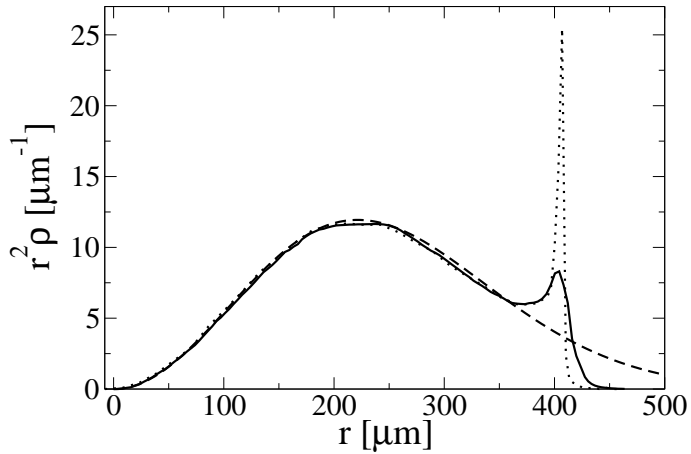


Figure 4: Spatial density  $\rho_i$  (solid) of the ions, at  $t = 3 \mu s$ , compared to the Gaussian profile assumed for the kinetic model (dashed). Additionally,  $\rho_i$  obtained from the particle simulation using the mean-field interaction only is shown as the dotted line. Initial-state parameters are the same as in fig. 1.

for the same plasma as in fig. 1. A mean-field treatment of the particle interactions [21] predicts that a shock front should form at the plasma edge, seen as the sharp spike in fig. 4 (dotted line). Apparently, with ionic correlations included (solid line) the peak structure is much less pronounced than in mean-field approximation. This is due to dissipation caused by ion-ion collisions which are fully taken into account in the HMD simulation. As shown in [32], by adding an ion viscosity term to the hydrodynamic equations of motion, dissipation tends to stabilize the ion density and prevents the occurrence of wavebreaking which was found to be responsible for the diverging ion density at the plasma edge in the case of a dissipationless plasma expansion. Furthermore, the initial correlation heating of the ions largely increases the thermal ion velocities, leading to a broadening of the peak structure compared to the zero-temperature case.

Another obvious aspect where ionic correlations play a dominant role is the behavior of the ionic temperature. Considering the huge ionic coupling constants suggested by the low initial ion temperatures, this temperature turns out to be an important quantity since it directly determines the value of  $\Gamma_i$ . According to a mean-field treatment, the ions would remain the (near) zero temperature fluid they are initially. However, as has been pointed out before, the ions are created in a completely uncorrelated non-equilibrium state, and they quickly heat up through the build-up of correlations as the system relaxes toward thermodynamical equilibrium. As shown in [14], even at early times the ionic velocity distribution is locally well described by a Maxwell distribution corresponding to a (spatially) local temperature, justifying the definition of a — due to the spherical symmetry of the plasma — radius-dependent ion temperature  $T_i(r, t)$ . Moreover, if the spatially averaged temperature is identified with the ion temperature determined by the model equations (2) one can find again good agreement between both approaches concerning the timescale of the initial heating as well as the magnitude of the ion temperature, even at later times [14]. However, as becomes apparent from fig. 5, the HMD simulations show temporal oscillations of the ionic temperature, which can, of course, not be described by the linear ansatz of the correlation-time approximation. Such temporal oscillations of the temperature during the initial relaxation stage are known from molecular dynamics simulations of homogeneous one-component [13] and two-component [33] plasmas, which are clearly caused by the strongly coupled collective

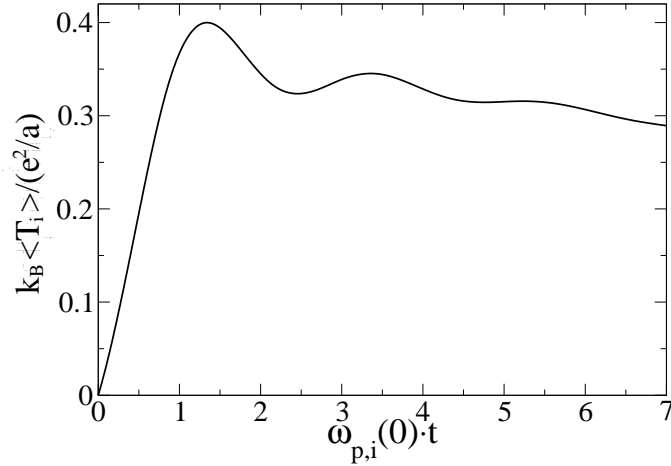


Figure 5: Time evolution of the density-scaled average ionic temperature for a plasma consisting of 400000 ions with an initial electronic Coulomb coupling parameter of  $\Gamma_e(0) = 0.07$ .

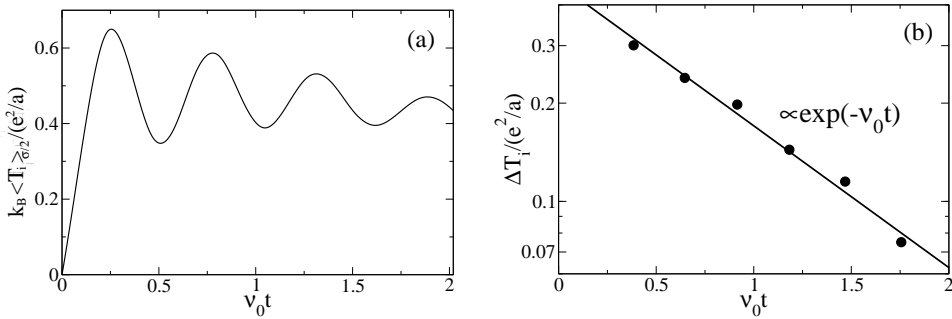


Figure 6: Time evolution of the ion temperature determined from a central sphere with a radius of half of the plasma width  $\sigma$  (a) and time dependence of the amplitude of the corresponding oscillations (b). The initial-state parameters are the same as in fig. 5.

ion dynamics, since they increase in strength with increasing  $\Gamma_i$  and disappear for  $\Gamma_i(0) < 0.5$  [13].

Despite the fact that the maximum initial coupling constant used in [13] is  $\Gamma_i = 5$ , while a value of  $\Gamma_i(0) \approx 40000$  is considered in the case of fig. 5, the oscillations observed in [13] are much more pronounced and persist much longer than in the present case. It becomes apparent that the rapid damping of the temperature oscillations can be traced to the inhomogeneity of the Gaussian density profile by looking at the central part of the plasma only, where the ionic density is approximately constant (figure 6). The temperature oscillations with an oscillation period of half of the inverse plasma frequency  $\nu_0 = \omega_{p,i}(0)/2\pi$  defined in the central plasma region are much more pronounced in this case, showing an exponential decay with a characteristic damping rate of  $\nu_0$  (fig. 6(b)). The temporally and spatially resolved temperature evolution shown in fig. 7 shows that the radially decreasing ion density leads to local temperature oscillations with radially increasing frequencies, thereby causing also spatial oscillations of the local ion temperature. Therefore, the seemingly enhanced damping rate, which has also been observed in recent experiments, is purely an effect of the averaging of these local oscillations over the total plasma



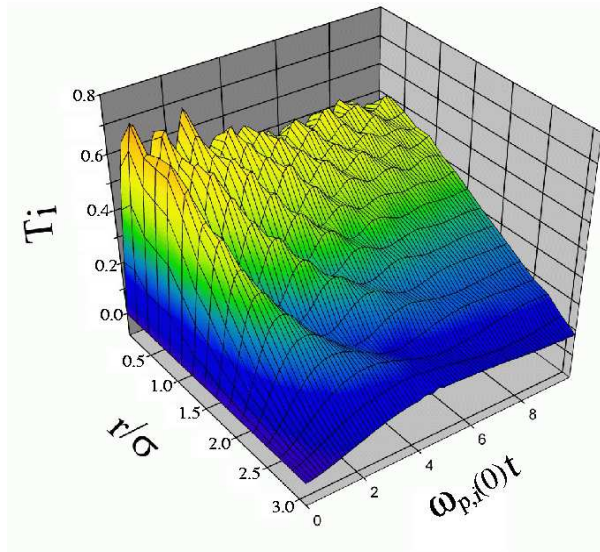


Figure 7: Temporally and spatially resolved time evolution of the ion temperature. The initial-state parameters are the same as in fig. 5.

volume.

### 3.3 Coulomb crystallization through laser cooling

The above considerations show that, while not dramatically affecting the overall expansion behavior of the plasma cloud, strong-coupling effects play an important role in different aspects of the evolution of UNPs. Thus, UNPs provide a prime example of laboratory realizations of strongly nonideal plasmas. Moreover, the HMD approach developed in [14] is well suited for an accurate description of these systems over experimentally relevant timescales, allowing for direct comparison between experiment and theory. Many interesting aspects of the relaxation behavior of these non-equilibrium plasmas may thus be studied in great detail. However, while effects of strong ionic coupling become apparent in UNPs, the naively expected regime with  $\Gamma > 100$  can not be reached with the current experimental setups. For the electrons, it is predominantly three-body recombination which heats them by several orders of magnitude, so that  $\Gamma_e < 0.2$  during the whole system evolution. The ionic component, on the other hand, is heated by the correlation-induced heating until  $\Gamma_i \approx 1$ , i.e. just at the border of the strongly coupled regime [29, 3]. Thus, it is the very build-up of ionic correlations one wishes to study that eventually shuts off the process and limits the amount of coupling achievable in these systems.

As soon as the reason for this ionic heating became clear, several proposals have been made in order to avoid or at least reduce the effect, among them *(i)* using fermionic atoms cooled below the Fermi temperature in the initial state, so that the Fermi hole around each atom prevents the occurrence of small interatomic distances [29]; *(ii)* an intermediate step of exciting atoms into high Rydberg states, so that the interatomic spacing is at least twice the radius of the corresponding Rydberg state [30]; and *(iii)* the continuous laser-cooling of the plasma ions after their initial creation, so that the correlation heating is counterbalanced by the external cooling [34, 24]. We have simulated the latter scenario using the HMD method, extended to allow for the description of laser cooling, as well as elastic electron-ion collisions which are negligible for the free plasma expansion but not necessarily in the laser-

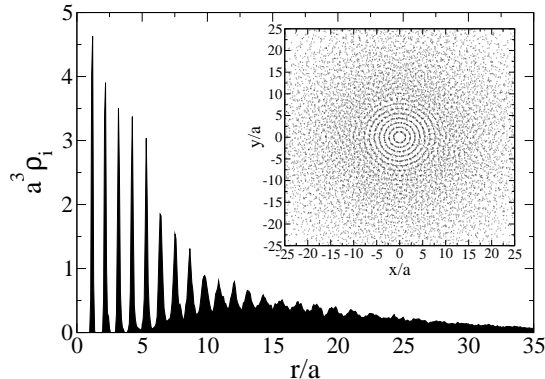


Figure 8: Radial density and a central slice of a plasma with  $N_i(0) = 80000$ ,  $\Gamma_e(0) = 0.08$ , cooled with a damping rate of  $\beta = 0.2\omega_{p,i}(0)$  at a time of  $\omega_{p,i}(0)t = 216$ . (For better contrast, different cuts have been overlaid.)

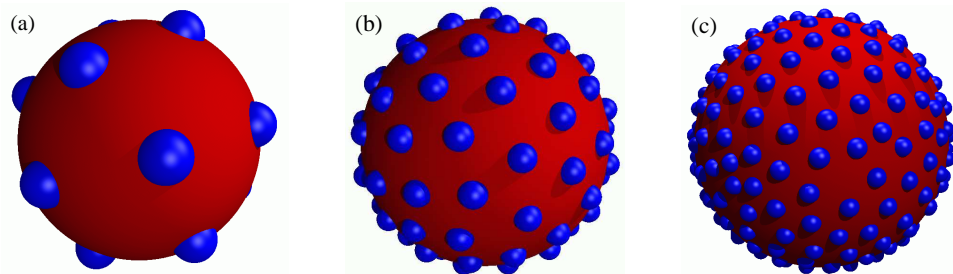


Figure 9: Arrangement of the ions on the first (a), third (b) and fifth (c) shell of the plasma of fig. 8.

cooled case [24, 22]. Laser cooling is modeled by adding a Langevin force

$$\mathbf{F}_{\text{cool}} = -m_i\beta\mathbf{v} + \sqrt{2\beta k_B T_c m_i}\boldsymbol{\xi} \quad (3)$$

to the ion equation of motion, where  $\mathbf{v}$  is the ion velocity,  $\boldsymbol{\xi}$  is a stochastic variable with  $\langle \boldsymbol{\xi} \rangle = \mathbf{0}$ ,  $\langle \boldsymbol{\xi}(t)\boldsymbol{\xi}(t+\tau) \rangle = 3\delta(\tau)$ , and the cooling rate  $\beta$  and the corresponding Doppler temperature  $T_c$  are determined by the properties of the cooling laser [35]. Elastic electron-ion collisions are taken into account on the basis of the corresponding Boltzmann collision integral, which is again evaluated by a Monte-Carlo procedure [22].

It is found that laser cooling leads to qualitative changes of the plasma dynamics. In particular, it significantly decelerates the expansion of the plasma, whose width is found to increase only as  $\sigma \propto t^{1/4}$ , in contrast to freely expanding plasmas which behave as  $\sigma \propto t$ . It is this drastic slow-down of the expansion which favors the development of strong ion correlations, compared to a free plasma where the expansion considerably disturbs the relaxation of the system. The simulations show further that strongly coupled expanding plasmas can indeed be created under realistic conditions, with ionic coupling constants far above the crystallization limit for homogeneous plasmas of  $\Gamma_i \approx 174$  [36]. Here we find, depending on the initial conditions, i.e. ion number and initial electronic Coulomb coupling parameter, strong liquid-like short-range correlations or even the onset of a radial crystallization of the ions. This is demonstrated in fig. 8, showing the radial density and a central slice of a plasma with  $N_i(0) = 80000$ ,  $\Gamma_e(0) = 0.08$ , cooled with a damping rate of  $\beta = 0.2\omega_{p,i}(0)$ , at a scaled time of  $\omega_{p,i}(0)t = 216$ . The formation of concentric

shells in the center of the cloud is clearly visible. As illustrated in fig. 9, beside the radial ordering there is also significant intra-shell ordering, namely a formation of hexagonal structures on the shells, which are, however, considerably disturbed by the curvature of the shells.

## 4 Conclusions

In summary, we have used an HMD approach to study the behavior of ultracold neutral plasmas on long time scales. We have shown that effects of strong interionic coupling are indeed visible in such systems, e.g. most prominently in the relaxation behavior of the ion temperature, which is connected with transient temporal as well as spatial oscillations. Nevertheless, the strongly coupled regime of  $\Gamma > 100$  is not reached with the current experimental setups. We have demonstrated, however, that additional continuous laser cooling of the ions during the plasma evolution qualitatively changes the expansion behavior of the system and should allow for the Coulomb crystallization of the plasma [24, 22]. It will be an interesting subject for further investigation to study in detail the dynamics of this crystallization process, which differs from the shell structure formation observed in trapped nonneutral plasmas [36] as explained in [24]. In particular, the influence of the plasma expansion, which presumably causes the transition from liquid-like short-range correlation to the radial ordering, deserves more detailed studies. Other future directions include the study of effects induced by additional magnetic fields, or of ways to confine the plasma in a trap.

We gratefully acknowledge many helpful discussions with J.M. Rost, as well as conversations with T.C. Killian and F. Robicheaux.

## References

- [1] T.C. Killian, S. Kulin, S.D. Bergeson, L.A. Orozco, C. Orzel and S.L. Rolston, Phys. Rev. Lett. **83**, 4776 (1999).
- [2] S. Kulin, T.C. Killian, S.D. Bergeson and S.L. Rolston, Phys. Rev. Lett. **85**, 318 (2000).
- [3] C.E. Simien, Y.C. Chen, P. Gupta, S. Laha, Y.N. Martinez, P.G. Mickelson, S.B. Nagel and T.C. Killian, Phys. Rev. Lett. **92**, 143001 (2004).
- [4] T.C. Killian, M.J. Lim, S. Kulin, R. Dumke, S.D. Bergeson and S.L. Rolston, Phys. Rev. Lett. **86**, 3759 (2001).
- [5] J.L. Roberts, C.D. Fertig, M.J. Lim and S.L. Rolston, Phys. Rev. Lett. **92**, 253003 (2004).
- [6] N. Vanhaecke, D. Comparat, D.A. Tate and P. Pillet, arXiv:physics/0401045
- [7] Yu.L. Klimontovich, Sov. Phys. JETP **35**, 920 (1972).
- [8] Yu.L. Klimontovich and W. Ebeling, Sov. Phys. JETP **36**, 476 (1973).
- [9] Yu.L. Klimontovich, *Kinetic theory of nonideal gases and nonideal plasmas* (Pergamon Press, 1982).
- [10] J. Wallenborn and M. Baus, Phys. Rev. A **18**, 1737 (1978).
- [11] V.V. Belyi, Yu.A. Kukharenko and J. Wallenborn, Phys. Rev. Lett. **76**, 3554 (1996).

- [12] M. Bonitz *Quantum Kinetic Theory* (Teubner, 1998).
- [13] G. Zwicknagel, *Contrib. Plasma Phys.* **39**, 155 (1999).
- [14] T. Pohl, T. Pattard and J.M. Rost, arXiv:physics/0405125 (2004).
- [15] Y. Hahn, *Phys. Lett. A* **293**, 266 (2002).
- [16] S.G. Kuzmin and T.M. O'Neil, *Phys. Rev. Lett.* **88**, 065003 (2002).
- [17] F. Robicieux and J.D. Hanson, *Phys. Rev. Lett.* **88**, 055002 (2002).
- [18] I.R. King, *Astron. J.* **71**, 64 (1966).
- [19] Yu.L. Klimontovich and D. Kremp, *Physica A* **109**, 517 (1981)
- [20] P. Mansbach and J. Keck, *Phys. Rev.* **181**, 275 (1969).
- [21] F. Robicieux and J.D. Hanson, *Phys. Plasmas* **10**, 2217 (2003).
- [22] T. Pohl, T. Pattard and J.M. Rost, *J. Phys. B* accepted (2004).
- [23] J.E. Barnes, *J. Comp. Phys.* **87**, 161 (1990).
- [24] T. Pohl, T. Pattard and J.M. Rost, *Phys. Rev. Lett.* **92**, 155003 (2004).
- [25] T. Pohl, T. Pattard and J.M. Rost, *J. Phys. B* **37**, L183 (2004).
- [26] D.S. Dorozhkina and V.E. Semenov, *Phys. Rev. Lett.* **81**, 2691 (1998).
- [27] M. Bonitz, *Phys. Lett. A* **221**, 85 (1996).
- [28] G. Chabrier and A.Y. Potekhin, *Phys. Rev. E* **58**, 4941 (1998).
- [29] M.S. Murillo, *Phys. Rev. Lett.* **87**, 115003 (2001).
- [30] D.O. Gericke and M.S. Murillo, *Contrib. Plasma Phys.* **43**, 298 (2003).
- [31] D.O. Gericke, M.S. Murillo, D. Semkat, M. Bonitz and D. Kremp, *J. Phys. A* **36** 6087 (2003).
- [32] C. Sack and H. Schamel, *Plasma Phys. Contr. F.* **27**, 717 (1985).
- [33] I.V. Morozov and G.E. Norman, *J. Phys. A* **36**, 6005 (2003).
- [34] T.C. Killian, V.S. Ashoka, P. Gupta, S. Laha, S.B. Nagel, C.E. Simien, S. Kulin, S.L. Rolston and S.D. Bergeson, *J. Phys. A* **36**, 6077 (2003).
- [35] H.J. Metcalf and P. van der Straten, *Laser Cooling and Trapping* (Springer, 1999).
- [36] D.H.E. Dubin and T.M. O'Neil, *Rev. Mod. Phys.* **71**, 87 (1999)